Synthesis, Properties, and Electrochemistry of bis(iminophosphorane)pyridine Iron(II) Pincer Complexes

Nicolás Sánchez López, Erick Nuñez Bahena, Alexander D Ryabov, Pierre Sutra, Alain Igau, Ronan Le Lagadec

inorganics

MDPI

Article

Synthesis, Properties, and Electrochemistry of bis(iminophosphorane)pyridine Iron(II) Pincer Complexes

Nicolás Sánchez López [1], Erick Nuñez Bahena [1], Alexander D. Ryabov [2], Pierre Sutra [3], Alain Igau [3] and Ronan Le Lagadec [1,*]

[1] Instituto de Química, Universidad Nacional Autónoma de México, Circuito Exterior s/n, Ciudad Universitaria, Ciudad de México 04510, Mexico; nicosanlop@comunidad.unam.mx (N.S.L.); ericknb@comunidad.unam.mx (E.N.B.)
[2] Department of Chemistry, Carnegie Mellon University, 4400 Fifth Avenue, Pittsburgh, PA 15213, USA; ryabov@andrew.cmu.edu
[3] CNRS, LCC (Laboratoire de Chimie, de Coordination), Université de Toulouse, CEDEX 4, 31077 Toulouse, France; pierre.sutra@lcc-toulouse.fr (P.S.); alain.igau@lcc-toulouse.fr (A.I.)
* Correspondence: ronan@unam.mx

Abstract: Iron derivatives have emerged as valuable catalysts for a variety of transformations, as well as for biological and photophysical applications, and iminophosphorane can be considered an ideal ligand scaffold for modulating electronic and steric parameters in transition metal complexes. In this report, we aimed to synthesize dichloride and dibromide iron(II) complexes supported by symmetric bis(iminophosphorane)pyridine ligands, starting from readily available ferrous halides. The ease of synthesis of this class of ligands served to access several derivatives with distinct electronic and steric properties imparted by the phosphine moiety. The ligands and the resulting iron(II) complexes were characterized by ^{31}P and ^{1}H NMR spectroscopy and DART or ESI mass spectrometry. While none of these iron(II) complexes could be characterized by single-crystal X-ray diffraction, suitable crystals of a μ-O bridged dinuclear iron complex bearing an iminophosphorane ligand were obtained, confirming a κ^3 binding motif. The bis(iminophosphorane)pyridine ligands in the obtained iron(II) complexes are labile, as demonstrated by their facile substitution by terpyridine. Cyclic voltammetry studies revealed that the oxidation of bis(iminophosphorane)pyridine iron(II) complexes to iron(III) species is quasi-reversible, suggesting the strong thermodynamic stabilization of the iron(III) center imparted by the σ-donating iminophosphorane ligands.

Keywords: pincer ligands; iminophosphorane ligand; iron; cyclic voltammetry

Citation: Sánchez López, N.; Nuñez Bahena, E.; Ryabov, A.D.; Sutra, P.; Igau, A.; Le Lagadec, R. Synthesis, Properties, and Electrochemistry of bis(iminophosphorane)pyridine Iron(II) Pincer Complexes. *Inorganics* **2024**, *12*, 115. https://doi.org/10.3390/inorganics12040115

Academic Editors: Sunčica Roca and Monika Kovačević

Received: 19 March 2024
Revised: 11 April 2024
Accepted: 11 April 2024
Published: 16 April 2024

1. Introduction

Iron complexes supported by 2,6-disubstituted pyridine pincer ligands have emerged as valuable catalysts for a variety of transformations, such as olefin polymerization and oligomerization, hydrogenation, and hydrofunctionalization reactions (Figure 1a) [1–3]. While, in some cases, the catalytic activity of these systems has been attributed to the redox-active nature of some of these ligands [4], it is generally accepted that adjusting the electronic properties at the metal center by ligand design is crucial for achieving optimal performance in catalysis [5]. Thus, developing new ligand sets in which ligand tuning can be easily accomplished is a challenging task. Diiminopyridine ligands are one of the most explored scaffolds for developing new transformations mediated or catalyzed by iron (Figure 1a, left). In considering this, we sought to access other types of easy-to-synthesize *N*,*N*,*N*-tridentate pincer ligands that could be suitable for tuning both the electronic and steric properties at the iron metal center [3,6].

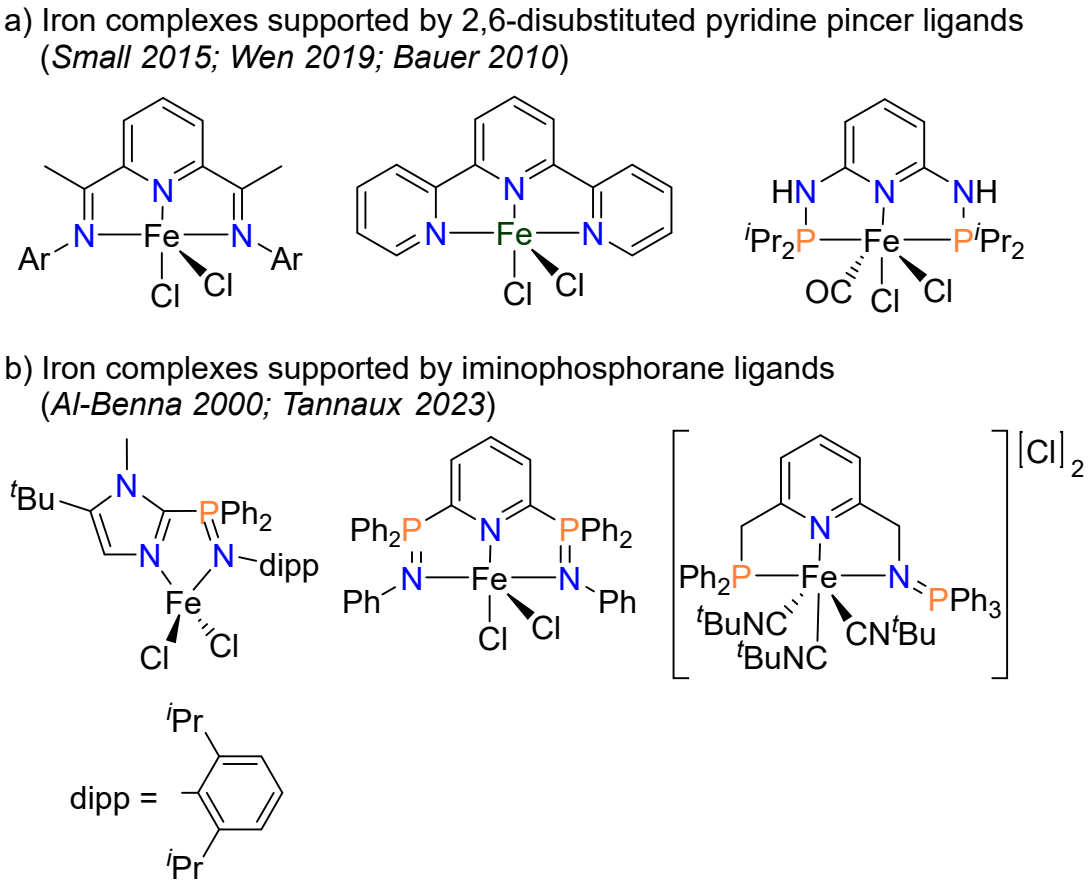

Figure 1. Examples of iron(II) pincer complexes and iminophosphorane iron(II) complexes [1–3,7,8].

Iminophosphoranes, the nitrogen analogs of phosphonium ylides, are suitable ligands for transition metal centers [6]. As shown in Scheme 1, the iminophosphorane motif is better represented by two canonical forms, one with phosphorus and nitrogen having a double bond $R_3P = NR'$ (ylene form) and the other with a single $R_3P^+–^-NR'$ bond with a positive charge on phosphorus and a negative charge on nitrogen (ylidic form). While experimental bond parameters support the depiction of iminophosphoranes as the $R_3P = NR'$ form (e.g., bond lengths of 1.54 Å–1.64 Å, and bond angles of 119°–143° in the solid-state) [9], DFT calculations indicate that the rotation energy of the P–N bond is only 2.1 kcal/mol, suggesting a significant contribution of the $R_3P^+–^-NR'$ form [10]. Due to the ylidic canonical form, iminophosphorane ligands are predominantly strong *σ N*-donors, resulting in convenient ligands to stabilize transition metal complexes in high oxidation states [11]. As the nature of the $R_3P = NR'$ partial double bonds involves negative hyperconjugation from a nitrogen lone pair p(N) to *s* *(P–C) orbitals [12,13], the σ-donor character of iminophosphoranes can be adjusted by the electronic properties of the phosphine moiety [11]. Consequently, iminophosphorane could be an ideal ligand scaffold for modulating electronic and steric parameters in transition metal complexes.

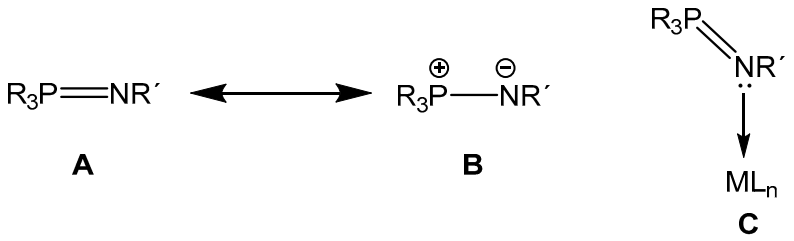

Scheme 1. Canonical forms of an iminophosphorane: ylene (**A**) and ylidic (**B**); its coordination to a metallic center (**C**).

While complexes supported by iminophosphorane ligands are common with lanthanides and early transition metals, examples of more electron-rich metal derivatives with iminophosphorane ligands have also been reported [6]. Iron catalysts bearing iminophosphoranes have been successfully employed for the activation of small molecules [14–16], as well as in ethylene oligomerization [17] and transfer hydrogenation [18].

As observed for other pincer ligands [19], tridentate ligands with one or two iminophosphorane fragments are less prone to engage in ligand substitution reactions than their bidentate and monodentate analogs, especially when bound to electron-rich metal centers [11]. In 2000, Bochmann and co-workers reported the synthesis of sterically hindered 2,6-bis(aryliminophosphoranyl)pyridine pincer complexes of vanadium, iron, cobalt, and nickel (e.g., Figure 1b, center) [7]. More recently, Auffrant and co-workers synthesized a related *P*,*N*,*N*-phosphine–pyridine–iminophosphorane iron pincer complex, which showed excellent catalytic activity in the hydrosilylation of acetophenones (Figure 1b) [8]. While these reports represent a significant advance toward using iminophosphoranes in the design of iron pincer complexes, their synthesis required the use of either $LiPR_2$ or Na/NH_3. Therefore, employing other pyridine iminophosphorane pincer ligands in designing iron coordination complexes that could be readily prepared from commercially available phosphines is highly desirable.

The *N*,*N*,*N*-pincer ligand bis(methyliminophosphoranyl)pyridine (**ImPh**, see Scheme 2a) is an ideal platform for stabilizing copper [20] and low-valent f elements [21,22]. In the case of copper, the coordination mode of **ImPh** depends on the oxidation state of the metal, with k^3-*N*,*N*,*N* and k^2-*N*,*N* coordination modes for Cu(II) and Cu(I) centers, respectively [20]. Due to the ease of synthesis of **ImPh**, which can be accessed from the corresponding organic diazide and triphenylphosphine, we hypothesized that other derivatives of this ligand scaffold could be obtained similarly using other phosphines. This would generate a set of ligands to modulate the electronic and steric properties of iron(II) pincer complexes. In addition, the potential of bis(iminophosphorane)pyridine ligands to exhibit hemilability could be advantageous for catalytic applications of the resulting iron complexes [20].

Herein, we report the synthesis of new bis(iminophosphorane)pyridine iron(II) pincer complexes. Their iminophosphorane ligands were effortlessly synthesized from commercially available phosphines. Reactivity studies of the complexes with terpyridine demonstrated the lability of the bis(iminophosphorane)pyridine ligands. The electronic properties of the new iron(II) complexes were evaluated by cyclic voltammetry.

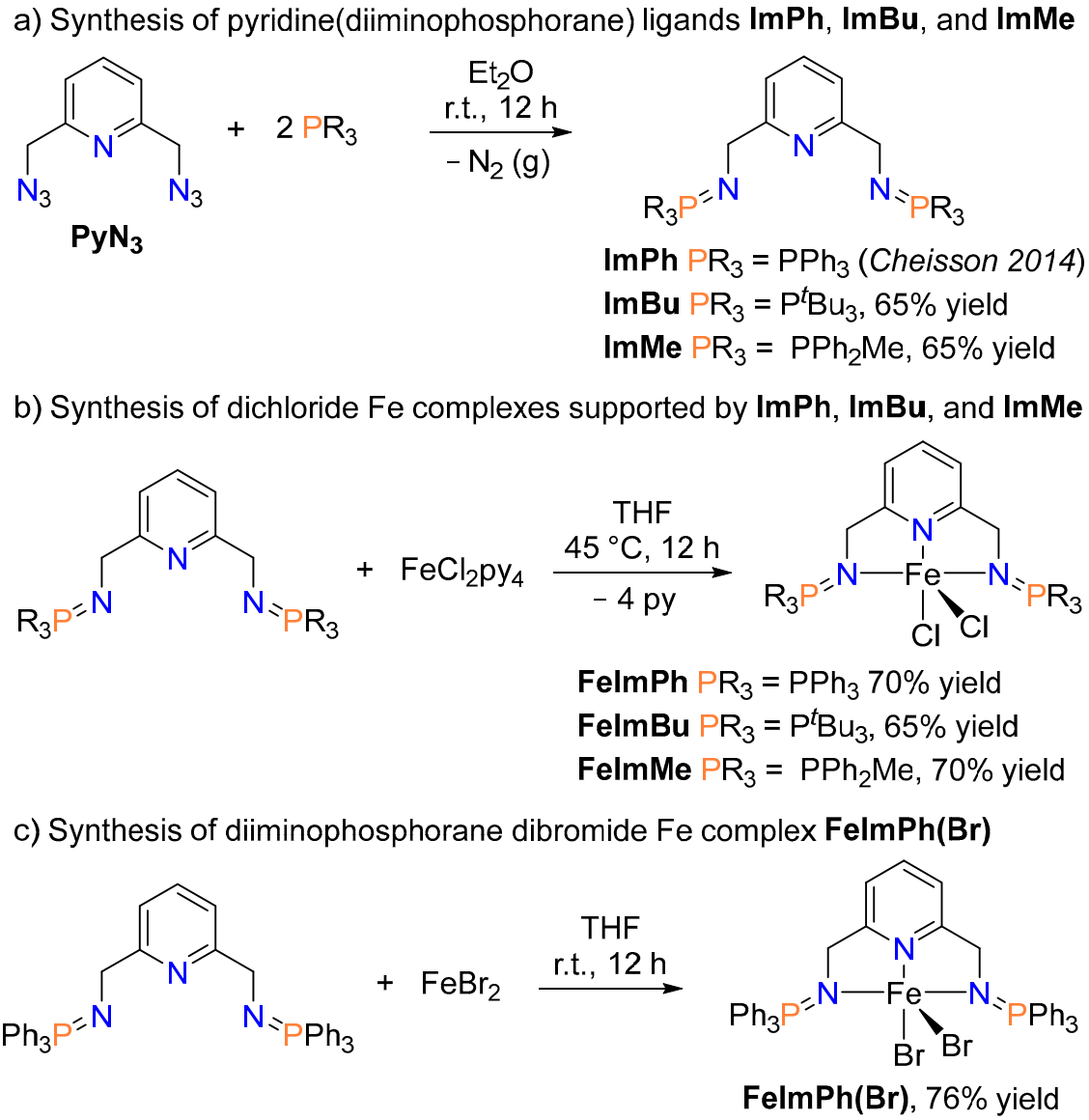

Scheme 2. Synthesis of bis(iminophosphorane)pyridine ligands and their iron(II) complexes [20].

2. Results and Discussion

2.1. Synthesis of Ligands and Iron Complexes

Iminophosphorane derivatives containing different phosphine moieties were synthesized analogously to the known **ImPh** ligand by the Staudinger reaction [20,23]. Accordingly, two equivalents of triphenylphosphine, tri-*tert*-butylphosphine, or diphenylmethylphosphine were added to a solution of 2,6-bis(azidomethyl)pyridine (**PyN3**) in diethyl ether and reacted overnight to obtain **ImPh** and new ligands **ImBu** and **ImMe**, respectively (Scheme 2a).

Iminophosphorane ligands **ImPh**, **ImBu**, and **ImMe** are white solids characterized by ^{1}H and ^{31}P NMR spectroscopy. In the ^{31}P NMR spectra, the resonances associated with the new ligands **ImBu** and **ImMe** appear as singlets at 53.65 and 12.85 ppm, respectively. In the ^{1}H NMR spectra, the methylene resonances of the iminophosphorane ligands appear as a singlet at 4.92 ppm for **ImBu** and as a broad doublet at 4.28 ppm for **ImMe**. Such differences observed in the multiplicity of the signal can be explained in terms of the electronic differences between the ligands **ImPh**, **ImMe**, and **ImBu**, which can lead to significant changes in the coupling constant values [24]. In the ATR-IR spectra, the band corresponding to N = P vibration is observed for **ImPh** at 1240 cm^{-1}, **ImBu** at 1109 cm^{-1}

and **ImMe at** 1223 cm^{-1}. The assignment of these structures was corroborated by MS (FAB+). The air and moisture-sensitive nature of ligands precluded their characterization by elemental analysis.

Next, the coordination of the iminophosphorane ligands to iron(II) was explored (Scheme 2b). The reaction of **ImPh** with $FeCl_2$ resulted in a complex reaction mixture, as observed by ^{31}P NMR spectroscopy. A yellow precipitate was formed when $FeCl_2py_4$ (py = pyridine) was employed as an iron precursor in the reaction with **ImPh** in THF at 45 °C for 12 h. In the ^{31}P NMR spectrum, the newly formed complex presented a characteristic singlet resonance at 38.64 ppm, which is significantly downfield shifted compared to that of the free ligand, thus supporting the coordination of **ImPh** to iron. The presence of only one signal in the ^{31}P NMR spectrum suggests a symmetric κ^3 binding mode in solution (Scheme 1b). When **ImBu** and **ImMe** independently reacted with $FeCl_2py_4$ under the same conditions, the formation of analog iron complexes was observed, as supported by the presence of singlet resonances in the ^{31}P NMR spectra (57.75 ppm for Fe**ImBu**, and 42.31 ppm for **FeImMe**). It should be noted that the presence of a small amount of paramagnetic impurity that could not be entirely removed causes the broadening of the ^1H NMR signals. In addition, the dibromide homolog **FeImPh(Br)** could be synthesized directly from $FeBr_2$ and **ImPh** at room temperature using a similar procedure (Scheme 2c). This is supported by the presence of a singlet signal at 42.31 ppm in the ^{31}P NMR spectrum of **FeImPh(Br)**, which is practically identical to that of the dichloride complex **FeImPh**. In the ATR-IR spectrum, the band corresponding to N = P vibration is observed at 1113 cm^{-1} for **FeImPh**, at 1173 cm^{-1} for **FeImBu**, at 1118 cm^{-1} for **FeImMe** and, at 1116 cm^{-1} for **FeImPh(Br)**. The structure of the synthesized bis(iminophosphorane)pyridine iron(II) complexes was corroborated by MS (DART) or MS (ESI). As mentioned for the free ligand, Fe**ImBu** is also highly sensitive to atmospheric conditions, precluding satisfactory elemental analysis [25]. Attempts to obtain MS data for Fe**ImBu** through different techniques such as DART+, FAB+, and ESI were unsuccessful.

Efforts to obtain crystalline material for X-ray diffraction of the bis(iminophosphorane) pyridine complexes under dry and air-free conditions were unsuccessful. Instead, suitable monocrystals of the μ-O-bridged dinuclear iron complex **Fe2ImPh** were obtained from a cold solution of **FeImPh** in THF (Scheme 3).

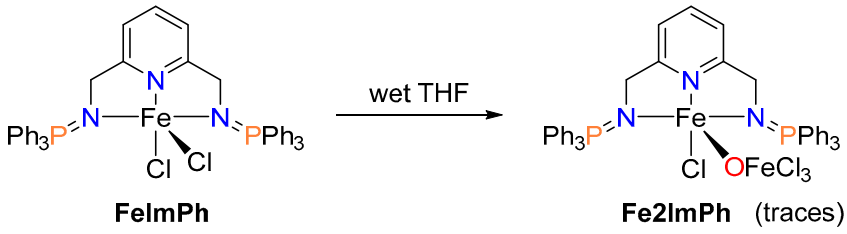

Scheme 3. Obtention of μ-oxo bridged dinuclear iron complex **Fe2ImPh** from **FeImPh**.

The **ImPh** ligand is part of a bimetallic unit with an oxygen bridge that links two iron atoms. This complex is obviously a minor byproduct. The bimetallic complex could form after the dissociation of **ImPh** from **FeImPh** to produce $FeCl_2$, followed by the oxidation of the latter by traces of dioxygen and the final association of a species produced with **FeImPh**. Bimetallic species **Fe2ImPh** contains a μ-oxo bridge that connects a $FeCl_3$ moiety with an iron center supported by the **ImPh** ligand. In the solid state of **Fe2ImPh** (Figure 2), the distances between the oxygen and the two iron centers are similar (Fe1−O1, 1.777(3) Å; Fe2−O1, 1.763(3) Å), suggesting a symmetrical binding mode of the *O*-donor. Analogous bimetallic μ-O-bridged iron species bearing (diimine)pyridine [26] and terpyridine [27] ligands have been reported. The three *N*-donor atoms of the bis(iminophosphorane)pyridine ligand are bound to Fe1 in a k^3 mode, as supported by bond distances (Fe1−N1, 2.098(4) Å; Fe1−N2, 2.134(4) Å; Fe1−N3, 2.132(4) Å). The parameter $\tau_5 = (\beta-\alpha)/60$, where β and α are the two greatest valence angles, was calculated [28]. The value $\tau_5 = 0.08$ confirmed

that the complex's geometry around Fe1 could be described as a distorted square pyramidal, with the **ImPh** ligand and the chloride atom in the plane and the $OFeCl_3$ unit in the axial position.

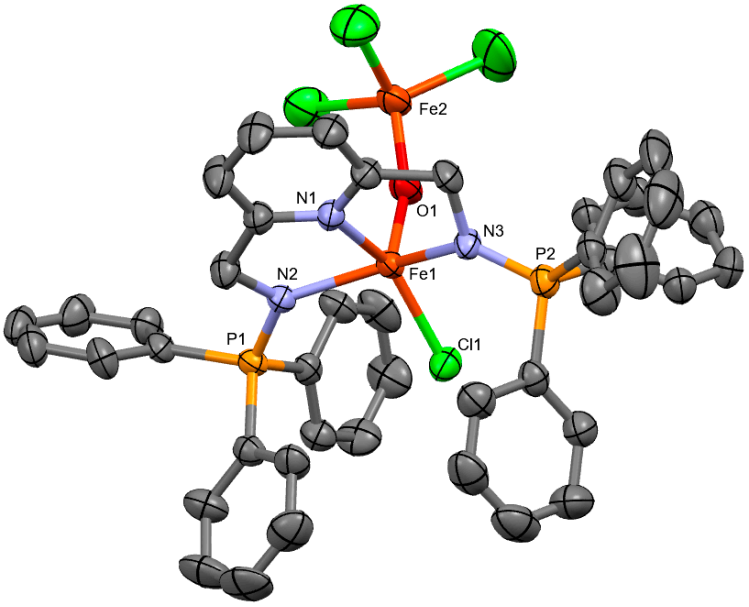

Figure 2. ORTEP representation of complex **Fe2ImPh** with ellipsoids is shown at 40% probability; hydrogen atoms are omitted for clarity. Selected bond lengths (Å) and angles (deg): Fe1−N1, 2.098(4); Fe1−N2, 2.134(4); Fe1−N3, 2.132(4); Fe1−O1, 1.777(3); Fe2−O1, 1.763(3); P1−N2, 1.610(4); P2−N3, 1.592(3); Fe1−O1−Fe2, 158.4(2).

The P−N bond distances in **Fe2ImPh** (P1−N2, 1.610(4) Å; P2−N3, 1.592(3) Å) are elongated with respect to the uncoordinated **ImPh** ligand (1.574(1) Å and 1.568(2) Å) [22]. This observation is consistent with the coordination of the nitrogen atoms of **ImPh** to the iron center.

2.2. Efforts toward the Synthesis of Heteroleptic Diiminophosphorane–Terpyridine Iron(II) Complexes

Octahedral ruthenium complexes with polypyridine ligands possess unique photophysical properties that have been broadly exploited [29–31]. While these complexes are the more studied group 8 metal compounds for this purpose, iron complexes have also been explored. Unfortunately, the metal-to-ligand charge transfer (MLCT) states of iron complexes are typically short-lived relative to those of the ruthenium analogs, thus translating into low quantum efficiencies [32]. Incorporating strong σ -donating ligands into an iron polypyridine fragment is an effective strategy for extending the lifetimes of MLCT states traditionally observed in polypyridine iron(II) complexes [32].

Within this context, several efforts were made to synthesize heteroleptic pyridine (diiminophosphorane)–terpyridine iron(II) complexes. When terpyridine (tpy) was introduced at room temperature to a solution or suspension of **FeImPh** in various organic solvents such as dichloromethane, methanol, acetonitrile, and THF, the bis(terpyridine)iron(II) complex $[Fe(tpy)_2]Cl_2$ was obtained as the major product, along with unreacted starting material, as observed by ^{31}P NMR. When this reaction was carried out under the same conditions with cationic iron(II) species formed in situ from **FeImPh** and different halogen abstracting agents such as $AgBF_4$, KPF_6, $TlPF_6$, and $NaBPh_4$, similar results were obtained (Scheme 4a). Starting from **FeImPh(Br)** led to similar results. For example, when terpyridine was reacted in THF with a cationic iron complex formed in situ from **FeImPh(Br)** and $NaBPh_4$ (room temperature, 12 h), $[Fe(tpy)_2][BPh_4]_2$ precipitated from the reaction mixture, while unreacted starting material remained in solution along with other uncharacterized

iron-containing species (Scheme 4b). X-ray diffraction studies of crystals of the material obtained from the soluble portion of this mixture revealed the formation of a terpyridine-diamine iron(II) complex [Fe(pyNH)(tpy)][BPh_4]$_2$ (Scheme 4b). However, the quality of the crystals was only sufficient for connectivity determination. We hypothesize that terpyridine heteroleptic complexes could be generated when the dissociated diiminophosphorane ligand is hydrolyzed by traces of water to form the corresponding primary amine, which could coordinate to a terpyridine-iron(II) fragment. However, more complex mechanisms involving reactive unsaturated iron intermediates cannot be ruled out.

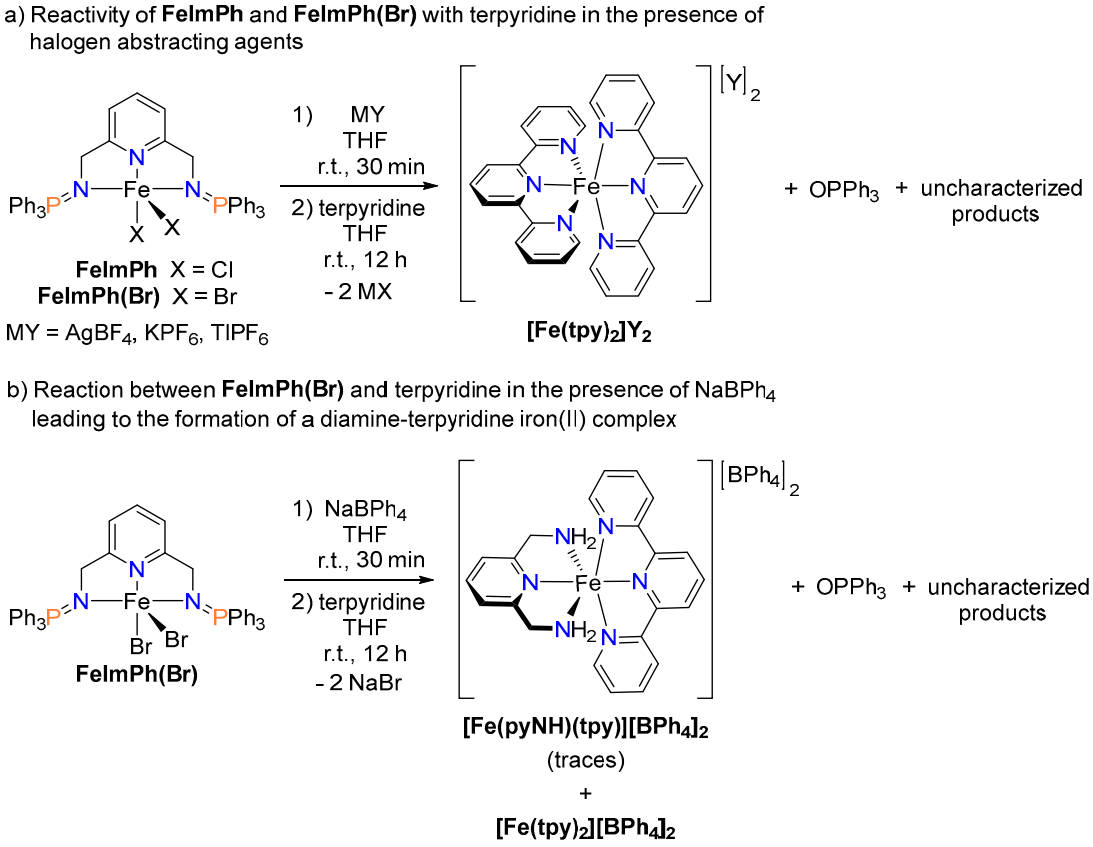

Scheme 4. Efforts toward the synthesis of a heteroleptic diiminophosphorane–terpyridine iron(II) complex.

Overall, these results highlight the lability of the diiminophosphorane ligand in these iron(II) complexes, which facilitates the formation of bis(terpyridine)-iron(II) complexes regardless of the reaction stoichiometry. Decoordination of the iminophosphorane ligand was similarly observed when bipyridine or monodentate ligands such as PPh_3 and CO were reacted with **FeImPh**. Such lability of our pincer ligands was not expected. However, the lability and hemilability of related ligands has previously been discussed [6,20,33].

2.3. Cyclic Voltammetry Studies

Redox properties of the synthesized bis(iminophosphorane)pyridine iron complexes were explored by cyclic voltammetry (CV). A quasi-reversible one-electron wave centered at $E_{1/2}$ = 0.103 V vs. Ag/AgCl was observed for **FeImPh** (Figure 3, right). This feature is tentatively assigned to a Fe(II)/Fe(III) couple. A similar quasi-reversible redox process centered at $E_{1/2}$ = 0.270 V vs. Ag/AgCl was observed for **FeImPh(Br)**. A slight potential shift was attributed to the more electron-donating nature of bromide with respect to chloride. For complexes **FeImBu** and **FeImMe**, almost irreversible redox waves centered around 0.62 and 0.05 V vs. Ag/AgCl, respectively, were observed. Other waves, probably

due to pyridine-centered events, were observed in the studied potential window of −2 to 2 V (Figure 3) [34].

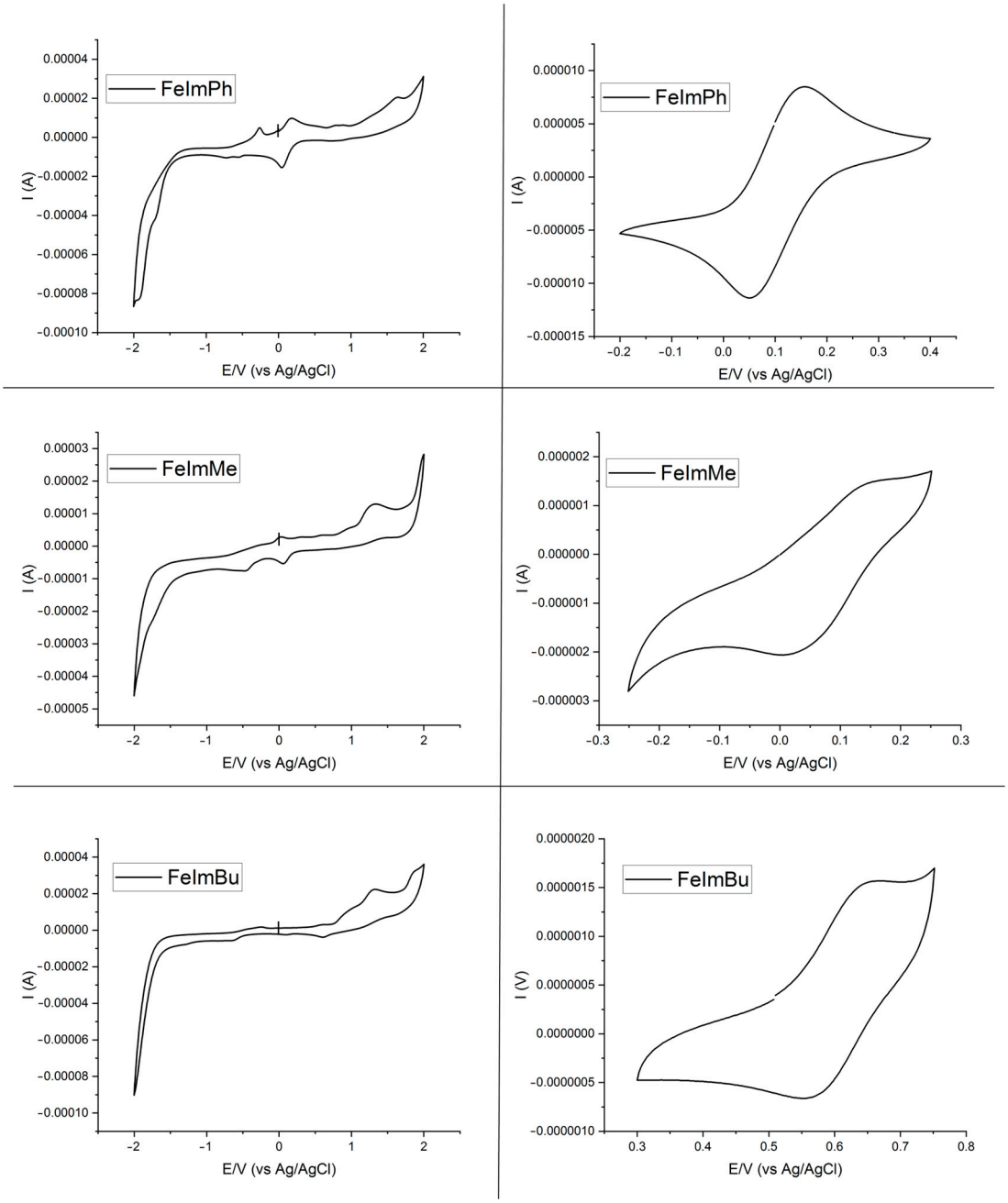

Figure 3. Cyclic voltammograms of complexes **FeImPh**, **FeImMe**, and **FeImBu** (0.1 M nBu$_4$NPF$_6$, 100 mVs^{-1}, glassy carbon, Ag/AgCl, 25 °C) in CH_2Cl_2 at 1×10^{-4} M.

3. Materials and Methods

3.1. Materials and Reagents

All reactions were carried out under a nitrogen atmosphere using standard Schlenk techniques. THF and Et_2O were distilled over sodium prior to use. Pyridine-2,6-dicarboxylic acid, $FeCl_2$, $FeBr_2$ Na_2CO_3, $NaBH_4$, PBr_3, PPh_3, PCH_3Ph_2, and tri-*tert*-butylphosphine solution (1.0 M in THF) were purchased from Sigma-Aldrich (St. Louis, MO, USA), and NaN_3 was purchased from MCF Productos Científicos (Hermosillo, Mexico). All purchased reagents were used as received. 2,6-bis(azidomethyl)pyridine and **ImPh** were prepared

according to the literature procedures [20]. The precursor $FeCl_2py_4$ was prepared following the literature procedures [35].

^1H, ^{13}C NMR, and ^{31}P NMR spectra were carried out on a JEOL GX 300 spectrometer (300.5296 MHz for ^1H, 75.5682 MHz for ^{13}C, and 121.5 MHz for ^{31}P). The δ scale was used throughout; chemical shifts were in ppm, and the coupling constants were in Hz. The samples of the iron complexes were prepared in an inert atmosphere and transferred to an NMR tube coupled to a J Young valve. FAB+ mass spectra were obtained using a JEOL JMS-SX102A instrument with *m*-nitrobenzyl alcohol as a matrix. DART mass spectra were obtained using the Joel AccuTOF JMS-T100LC instrument. Infrared spectra were performed on a Bruker Alpha ATR spectrometer. A three-electrode configuration was used with a BAS working glassy carbon electrode, Ag/AgCl reference electrode, and auxiliary Pt electrode. Before each measurement, the working electrode was polished with a diamond paste and rinsed with acetone and distilled water. All potential scans were carried out at a scanning rate of 100 mVs^{-1} in dry CH_2Cl_2 at a concentration of 1×10^{-4} M and 0.1 M of tetra-*n*butylammonium hexafluorophosphate. Under those conditions, $E_{1/2}$ = 0.494 V (vs. Ag/AgCl) for the ferrocene/ferrocenium redox couple.

Crystallography. Dark brown crystals of **Fe2ImPh** were obtained by cooling a THF solution of **FeImPh** to 0 °C for two days. The X-ray intensity data were measured at 298(2) K on a Bruker Smart Apex CCD diffractometer using standard MoKα radiation (λ = 0.71073 Å). A multi-scan absorption correction procedure was applied. The integration of the data was done using a triclinic unit cell to yield a total of 13654 reflections to a maximum 2θ angle of 51.06°, of which 9594 [R(int) = 0.0739] were independent. The integration structure solution was performed using SHELXS-2012, and refinement (full-matrix least squares) was performed using the SHELXS-2014/7 program [36]. Hydrogen atoms were placed in calculated positions and were allowed to ride on the atoms to which they were attached. Crystal structure parameters and experimental data on the structure solution and refinement are given in Table S10 in Supporting Information.

3.2. Synthesis of ***ImBu***

In a Schlenk flask, 0.214 g (1.056 mmol) of tri-*tert*-butylphosphine were slowly added to a solution of 0.10 g (0.528 mmol) of 2,6-bis(azidomethyl)pyridine in 10 mL of dry diethyl ether, and the reaction mixture was stirred at room temperature for 12 h. The solvent was concentrated under a vacuum to about 5 mL, and the white precipitate was filtered off through a cannula fitted with filter paper, then washed with 30 mL of cold hexane and dried under a vacuum. The white solid corresponding to **ImBu** was obtained in 65% yield (0.225 g, 0.343 mmol).

$^{31}P\{^1H\}$ NMR ($CDCl_3$, 121 MHz) 53.65 (s). ^1H NMR ($CDCl_3$, 300 MHz) 7.44 (t, 1H), 7.17 (d, J_{HH} = 9.0, 2H), 4.92 (s, 4H), 1.43 (d, J_{PH} = 12.0, 54H). IR (ν cm^{-1}): 1109 ($\nu_{N=P}$).

3.3. Synthesis of ***ImMe***

In a Schlenk flask, 0.211 g (1.056 mmol) of methyldiphenylphosphine were slowly added to a solution of 0.10 g (0.528 mmol) of 2,6-bis(azidomethyl)pyridine in 10 mL of diethyl ether, and the reaction mixture was stirred at room temperature for 12 h. The solvent was concentrated under a vacuum to about 5 mL, and the white precipitate was filtered off through a cannula fitted with filter paper, then washed with 30 mL of cold diethyl ether and dried under a vacuum. The white solid corresponding to **ImMe** was obtained in 65% yield (0.168 g, 0.316 mmol).

$^{31}P\{^1H\}$ NMR ($CDCl_3$, 121 MHz) 12.85 (s). ^1H NMR ($CDCl_3$, 300 MHz) 7.66–7.54 (m, 12H, H1, H2, H6), 7.42–7.31 (m, 13H, H7, H8), 4.28 (d, J_{PH} = 21.0, 4H, H4) 1.91 (d, J_{PH} = 12.0, 6H, H9). MS(DART) *m/z* Calcd for $C_{33}H_{33}N_3P_2$ $[M+H]^+$: 533.60; found: 534. See Figure S5 for compound numeration.

*3.4. Synthesis of **FeImPh***

In a Schlenk flask, 0.067 g, (0.152 mmol) of $FeCl_2py_4$ were added to a solution of 0.10 g (0.152 mmol) of **ImPh** in 20 mL of dry THF. The reaction mixture was stirred for 12 h at 45 °C. The brown precipitate was obtained and filtered through a cannula fitted with filter paper under a nitrogen atmosphere. The brown solid was dissolved in 15 mL of CH_2Cl_2 and filtered through a cannula fitted with filter paper. The solvent was evaporated to dryness, and the dark residue was dissolved in 100 mL of acetone, filtered through a short plug of Celite®, and the solvent was evaporated to dryness. The yellow solid was washed with 30 mL of diethyl ether and dried under vacuum to give the compound **FeImPh** in 70% yield (0.083 g, 0.106 mmol).

$^{31}P\{^1H\}$ NMR ($CDCl_3$, 121 MHz) 38.64 (s). ^1H NMR ($CDCl_3$, 300 MHz) 7.45–7.90 (m, 34H, H1, H2, H6, H7, H8), 4.15 (d, J_{PH} = 18, 4H, H4). See Figure S6 for compound numeration. MS(ESI+) *m/z* Calcd for $C_{43}H_{37}C_{l2}FeN_3P_2$ [M]+: 783.12; found: 783.60. IR (ν cm^{-1}): 1113 ($\nu_{N=P}$). Anal Calcd for $C_{43}H_{37}C_{l2}FeN_3P_2 \cdot 0.7\ CH_2Cl_2$: N, 4.98; C, 62.19; H, 4.59. Found: N, 5.21; C, 62.03; H, 4.69.

*3.5. Synthesis of **FeImBu***

In a Schlenk flask, 0.10 g, (0.186 mmol) of $FeCl_2py_4$ were added to a solution of 0.10 g (0.152 mmol) of **ImBu** in 20 mL of dry THF. The reaction mixture was stirred for 12 h at 45 °C. The brown precipitate was obtained and filtered through a cannula fitted with filter paper. The brown solid was dissolved in 15 mL of CH_2Cl_2 and filtered through a cannula fitted with filter paper. The solvent was evaporated to dryness, and the dark residue was dissolved in 100 mL of acetone, filtered through a short plug of Celite®, and the solvent was evaporated to dryness. The yellow solid was washed with 30 mL of diethyl ether and dried under vacuum to give the compound **FeImBu** in 65% yield (0.080 g, 0.120 mmol).

$^{31}P\{^1H\}$ NMR ($CDCl_3$, 121 MHz) 57.75 (s). ^1H NMR ($CDCl_3$, 300 MHz) 7.70–7.41 (m, 3H), 5.36 (m, 4H), 1.68–1.04 (m, 54 H). IR (ν cm^{-1}): 1144 ($\nu_{N=P}$). See Figure S7 for compound numeration. Satisfactory elemental analysis could not be obtained due to the high air and moisture-sensitive nature of this complex.

*3.6. Synthesis of **FeImMe***

In a Schlenk flask, 0.083 g (0.187 mmol) of $FeCl_2py_4$ were added to a solution of 0.10 g (0.187 mmol) of **ImMe** in 20 mL of dry THF. The reaction mixture was stirred for 12 h at 45 °C. The brown precipitate was obtained and filtered through a cannula fitted with filter paper. The brown solid was dissolved in 15 mL of CH_2Cl_2 and filtered through a cannula fitted with filter paper. The solvent was evaporated to dryness, and the dark residue was dissolved in 100 mL acetone, filtered through a short plug of Celite®, and the solvent was evaporated to dryness. The yellow solid was washed with 30 mL of diethyl ether and dried under vacuum to give the compound **FeImMe** in 70% yield (0.086 g, 0.130 mmol).

$^{31}P\{^1H\}$ NMR ($CDCl_3$, 121 MHz) 42.31 (s). ^1H NMR ($CDCl_3$, 300 MHz) 7.81–7.47 (m, 23H, H1, H2, H3, H6, H7, H8), 4.19 (m, 4H, H4), 2.66 (m, 6H, CH_3). See Figure S8 for compound numeration. MS(DART) *m/z* Calcd for $C_{33}H_{33}C_{l2}FeN_3P_2$ $[M+H]^+$: 660.09; found: 660. IR (ν cm^{-1}): 1118 ($\nu_{N=P}$). Anal Calcd for $C_{33}H_{33}Cl_2FeN_3P_2 \cdot 0.8\ CH_2Cl_2$: N, 5.77; C, 55.74; H, 4.79. Found: N, 6.57; C, 55.06; H, 5.00.

*3.7. Synthesis of **FeImPh(Br)***

In a Schlenk flask, 0.039 g (0.182 mmol) of $FeBr_2$ were added to a solution of 0.12 g (0.182 mmol) of **ImPh** in 20 mL of dry THF. The reaction mixture was stirred for 12 **h** at room temperature. After this time, a yellow precipitate was obtained and filtered through a cannula fitted with filter paper. This solid was washed with 30 mL of cold THF and dried under vacuum to give the compound **FeImPh(Br)** as a yellow solid in 76% yield (0.121 g, 0.138 mmol).

$^{31}P\{^{1}H\}$ NMR ($CDCl_3$, 121 MHz) 42.31 (s). ^{1}H NMR ($CDCl_3$, 300 MHz) 8.61 (s, 4H) 7.73–7.28 (m, 27H), 6.24 (s, 2H), 4.22 (s, 4H). MS(ESI+) *m/z* Calcd for $C_{43}H_{37}Br_2FeN_3P_2$ $[M+H]^+$: 874.02; found: 874.2. IR (ν cm^{-1}): 1116 ($\nu_{N=P}$).

*3.8. Reaction between **FeImPh** and terpyridine*

In a typical reaction, 0.1 g (0.127 mmol) of **FeImPh** were added to a solution of 0.029 g (0.127 mmol) of terpyridine in 20 mL of dry solvent in a Schlenk flask. The reaction mixture was stirred at room temperature. The purple solution was evaporated to dryness under vacuum, and the residue was dissolved in 15 mL of CH_2Cl_2. Upon chromatography through a short column of alumina, two fractions were obtained. A yellow fraction contained mainly unreacted **FeImPh**, while the purple fractions contained $[Fe(tpy)_2]Cl_2$. After the evaporation of the solvent, the purple solid was washed with 20 mL of diethyl ether and dried under vacuum, leading to $[Fe(tpy)_2]Cl_2$ in yields from 15% to 25%, depending on the reaction time and solvent.

^{1}H NMR ($CDCl_3$, 300 MHz) 7.69–7.62 (m, 8H), 7.57–7.51 (m, 5H), 7.48–7,42 (m, 9H). See Figure S12 in Supporting Information.

4. Conclusions

Pyridine(diiminophosphoranes) are convenient ligands for accessing iron(II) coordination complexes. The methodology developed here allows for the easy preparation of various bis(iminophosphorane)pyridine complexes of iron(II). Their electronic and steric properties can be tuned by the phosphine ligand, which can be incorporated into the iminophosphorane framework through a straightforward synthetic procedure. We hypothesize that such iron(II) bis(iminophosphorane)pyridine complexes are candidates for catalytic processes known to be catalyzed by other iron(II) pincer complexes.

Supplementary Materials: The following supporting information can be downloaded at: https://www.mdpi.com/article/10.3390/inorganics12040115/s1: Synthesis and characterization of **PyN3** and **ImPh** (S2–S3); IR, ^{1}H- and ^{31}P-NMR spectra, IR, M/S data, and cyclic voltammogram for **IMBu**, **ImMe**, **FeImPh**, **FeImBu**, **FeImMe**, and **FeImPh(Br)** (S4–S9); Crystallographic details for **Fe2ImPh** (S10); Studies of the stability of **FeImPh** and **FeImBu** in solution (S11); NMR spectra for $[Fe(tpy)_2]Cl_2$ and $OPPh_3$ (S12); CV of ferrocene in CH_2Cl_2 (S13). CCDC 2332976 for **Fe2ImPh** contains the supplementary crystallographic data for this paper. These data can be obtained free of charge from The Cambridge Crystallographic Data Centre.

Author Contributions: Conceptualization, N.S.L., A.I. and R.L.L.; methodology, N.S.L., E.N.B. and R.L.L.; investigation, N.S.L., E.N.B. and R.L.L.; writing—original draft preparation, N.S.L., E.N.B. and R.L.L.; writing—review and editing, P.S., A.I., A.D.R. and R.L.L.; funding acquisition, R.L.L. All authors have read and agreed to the published version of the manuscript.

Funding: This research was funded by DGAPA—UNAM (PAPIIT projects IN-207419 and IN-211522) and Consejo Nacional de Humanidades, Ciencia y Tecnología CONAHCYT (Project A1-S-15068, and grant to N. Sánchez López).

Data Availability Statement: The data presented in this study are available in the article and Supplementary Materials.

Acknowledgments: Rubén A. Toscano and Marcos Flores-Álamo are thanked for X-rya diffraction studies. We thank M. P. Orta Perez, E. Huerta Salazar, E. García Ríos, R. L. Gaviño Ramirez, J. D. Vázquez Cuevas, M. M. Aguilar Araiza, and G. E. Cortés Romero for obtaining analytical data and for technical assistance. J. F. Zambrano Bedoya is thanked for his help in evaluating the stability of the compounds.

Conflicts of Interest: The authors declare no conflicts of interest.

References

1. Small, B.L. Discovery and Development of Pyridine-bis(imine) and Related Catalysts for Olefin Polymerization and Oligomerization. *Acc. Chem. Res.* **2015**, *48*, 2599–2611. [CrossRef] [PubMed]
2. Wen, H.; Liu, G.; Huang, Z. Recent advances in tridentate iron and cobalt complexes for alkene and alkyne hydrofunctionalizations. *Coord. Chem. Rev.* **2019**, *386*, 138–153. [CrossRef]
3. Bauer, G.; Hu, X. Recent developments of iron pincer complexes for catalytic applications. *Inorg. Chem. Front.* **2016**, *3*, 741–765. [CrossRef]
4. Tondreau, A.M.; Milsmann, C.; Patrick, A.D.; Hoyt, H.M.; Lobkovsky, E.; Wieghardt, K.; Chirik, P.J. Synthesis and Electronic Structure of Cationic, Neutral, and Anionic Bis(imino)pyridine Iron Alkyl Complexes: Evaluation of Redox Activity in Single-Component Ethylene Polymerization Catalysts. *J. Am. Chem. Soc.* **2010**, *132*, 15046–15059. [CrossRef] [PubMed]
5. Arevalo, R.; Chirik, P.J. Enabling Two-Electron Pathways with Iron and Cobalt: From Ligand Design to Catalytic Applications. *J. Am. Chem. Soc.* **2019**, *141*, 9106–9123. [CrossRef] [PubMed]
6. García-Álvarez, J.; García-Garrido, S.E.; Cadierno, V. Iminophosphorane–phosphines: Versatile ligands for homogeneous catalysis. *J. Organomet. Chem.* **2014**, *751*, 792–808. [CrossRef]
7. Al-Benna, S.; Sarsfield, M.J.; Thornton-Pett, M.; Ormsby, D.L.; Maddox, P.J.; Brès, P.; Bochmann, M. Sterically hindered iminophosphorane complexes of vanadium, iron, cobalt and nickel: A synthetic, structural and catalytic study †. *J. Chem. Soc. Dalton Trans.* **2000**, 4247–4257. [CrossRef]
8. Tannoux, T.; Mazaud, L.; Cheisson, T.; Casaretto, N.; Auffrant, A. Fe(II) complexes supported by an iminophosphorane ligand: Synthesis and reactivity. *Dalton Trans.* **2023**, *52*, 12010–12019. [CrossRef] [PubMed]
9. Sudhakar, P.V.; Lammertsma, K. Nature of bonding in phosphazoylides. A comparative study of N2H4, NPH4, and P2H4. *J. Am. Chem. Soc.* **2002**, *113*, 1899–1906. [CrossRef]
10. Molina, P.; Alajarin, M.; Lopez Leonardo, C.; Claramunt, R.M.; Foces-Foces, M.d.l.C.; Hernandez Cano, F.; Catalan, J.; De Paz, J.L.G.; Elguero, J. Experimental and theoretical study of the R3P+-X- bond. Case of betaines derived from N-iminophosphoranes and alkyl isocyanates. *J. Am. Chem. Soc.* **2002**, *111*, 355–363. [CrossRef]
11. Tannoux, T.; Auffrant, A. Complexes featuring tridentate iminophosphorane ligands: Synthesis, reactivity, and catalysis. *Coord. Chem. Rev.* **2023**, *474*, 214845. [CrossRef]
12. Chaplin, A.B.; Harrison, J.A.; Dyson, P.J. Revisiting the Electronic Structure of Phosphazenes. *Inorg. Chem.* **2005**, *44*, 8407–8417. [CrossRef] [PubMed]
13. Reed, A.E.; Schleyer, P.v.R. Chemical bonding in hypervalent molecules. The dominance of ionic bonding and negative hyperconjugation over d-orbital participation. *J. Am. Chem. Soc.* **2002**, *112*, 1434–1445. [CrossRef]
14. Winslow, C.; Lee, H.B.; Field, M.J.; Teat, S.J.; Rittle, J. Structure and Reactivity of a High-Spin, Nonheme Iron(III)- Superoxo Complex Supported by Phosphinimide Ligands. *J. Am. Chem. Soc.* **2021**, *143*, 13686–13693. [CrossRef] [PubMed]
15. Hein, N.M.; Pick, F.S.; Fryzuk, M.D. Synthesis and Reactivity of a Low-Coordinate Iron(II) Hydride Complex: Applications in Catalytic Hydrodefluorination. *Inorg. Chem.* **2017**, *56*, 14513–14523. [CrossRef] [PubMed]
16. Spentzos, A.Z.; May, S.R.; Confer, A.M.; Gau, M.R.; Carroll, P.J.; Goldberg, D.P.; Tomson, N.C. Investigating Metal-Metal Bond Polarization in a Heteroleptic Tris-Ylide Diiron System. *Inorg. Chem.* **2023**, *62*, 11487–11499. [CrossRef] [PubMed]
17. Spencer, L.P.; Altwer, R.; Wei, P.; Gelmini, L.; Gauld, J.; Stephan, D.W. Pyridine− and Imidazole−Phosphinimine Bidentate Ligand Complexes: Considerations for Ethylene Oligomerization Catalysts. *Organometallics* **2003**, *22*, 3841–3854. [CrossRef]
18. Oheix, E.; Herrero, C.; Moutet, J.; Rebilly, J.N.; Cordier, M.; Guillot, R.; Bourcier, S.; Banse, F.; Senechal-David, K.; Auffrant, A. Fe(III) and Fe(II) Phosphasalen Complexes: Synthesis, Characterization, and Catalytic Application for 2-Naphthol Oxidative Coupling. *Chemistry* **2020**, *26*, 13634–13643. [CrossRef]
19. Peris, E.; Crabtree, R.H. Key factors in pincer ligand design. *Chem. Soc. Rev.* **2018**, *47*, 1959–1968. [CrossRef]
20. Cheisson, T.; Auffrant, A. Versatile coordination chemistry of a bis(methyliminophosphoranyl)pyridine ligand on copper centres. *Dalton Trans.* **2014**, *43*, 13399–13409. [CrossRef]
21. Cheisson, T.; Ricard, L.; Heinemann, F.W.; Meyer, K.; Auffrant, A.; Nocton, G. Synthesis and Reactivity of Low-Valent f-Element Iodide Complexes with Neutral Iminophosphorane Ligands. *Inorg. Chem.* **2018**, *57*, 9230–9240. [CrossRef]
22. Cheisson, T.; Auffrant, A.; Nocton, G. η5–η1 Switch in Divalent Phosphaytterbocene Complexes with Neutral Iminophosphoranyl Pincer Ligands: Solid-State Structures and Solution NMR 1JYb–P Coupling Constants. *Organometallics* **2015**, *34*, 5470–5478. [CrossRef]
23. Staudinger, H.; Meyer, J. Über neue organische phosphorverbindungen III. Phosphinmethylenderivate und phosphinimine. *Helv. Chim. Acta* **1919**, *2*, 635–646. [CrossRef]
24. Gorenstein, D.G. Conformation and Dynamics of DNA and Protein-DNA Complexes by 31P NMR. *Chem. Rev.* **1994**, *94*, 1315–1338. [CrossRef]
25. Kuveke, R.E.H.; Barwise, L.; van Ingen, Y.; Vashisth, K.; Roberts, N.; Chitnis, S.S.; Dutton, J.L.; Martin, C.D.; Melen, R.L. An International Study Evaluating Elemental Analysis. *ACS Cent. Sci.* **2022**, *8*, 855–863. [CrossRef]
26. Small, B.L.; Brookhart, M. Polymerization of propylene by a new generation of iron catalysts: Mechanisms of chain initiation, propagation, and termination. *Macromolecules* **1999**, *32*, 2120–2130. [CrossRef]
27. Bocian, A.; Napierała, S.; Gorczyński, A.; Kubicki, M.; Wałęsa-Chorab, M.; Patroniak, V. The first example of an asymmetrical μ-oxo bridged dinuclear iron complex with a terpyridine ligand. *New J. Chem.* **2019**, *43*, 12650–12656. [CrossRef]

28. Addison, A.W.; Rao, T.N.; Reedijk, J.; van Rijn, J.; Verschoor, G.C. Synthesis, structure, and spectroscopic properties of copper(II) compounds containing nitrogen–sulphur donor ligands; the crystal and molecular structure of aqua [1,7-bis(N-methylbenzimidazol-2′-yl)-2,6-dithiaheptane]copper(II) perchlorate. *J. Chem. Soc. Dalton Trans.* **1984**, *7*, 1349–1356. [CrossRef]
29. Hagfeldt, A.; Boschloo, G.; Sun, L.; Kloo, L.; Pettersson, H. Dye-sensitized solar cells. *Chem. Rev.* **2010**, *110*, 6595–6663. [CrossRef]
30. Prier, C.K.; Rankic, D.A.; MacMillan, D.W. Visible light photoredox catalysis with transition metal complexes: Applications in organic synthesis. *Chem. Rev.* **2013**, *113*, 5322–5363. [CrossRef]
31. Lebon, E.; Bastin, S.; Sutra, P.; Vendier, L.; Piau, R.E.; Dixon, I.M.; Boggio-Pasqua, M.; Alary, F.; Heully, J.-L.; Igau, A. Can a functionalized phosphine ligand promote room temperature luminescence of the [Ru (bpy)(tpy)] 2+ core? *Chem. Commun.* **2012**, *48*, 741–743. [CrossRef]
32. Liu, Y.; Persson, P.; Sundstrom, V.; Warnmark, K. Fe N-heterocyclic carbene complexes as promising photosensitizers. *Acc. Chem. Res.* **2016**, *49*, 1477–1485. [CrossRef]
33. Fukui, M.; Itoh, K.; Ishii, Y. Iminophosphorane Complexes of Palladium(II). *Bull. Chem. Soc. Jpn.* **1975**, *48*, 2044–2046. [CrossRef]
34. Martin, D.J.; McCarthy, B.D.; Piro, N.A.; Dempsey, J.L. Synthesis and electrochemical characterization of a tridentate Schiff-base ligated Fe(II) complex. *Polyhedron* **2016**, *114*, 200–204. [CrossRef]
35. Wu, J.Y.; Stanzl, B.N.; Ritter, T. A strategy for the synthesis of well-defined iron catalysts and application to regioselective diene hydrosilylation. *J. Am. Chem. Soc.* **2010**, *132*, 13214–13216. [CrossRef]
36. Sheldrick, G.M. Crystal structure refinement with SHELXL. *Acta Crystallogr. Sect. C Struct. Chem.* **2015**, *71*, 3–8. [CrossRef]